

Spectral beam compression and combination using fiber laser sources

Sean Moore, Daniel Soh, Kevin Schroder, and Wen Hsu
 Sandia National Laboratories, P.O. Box 969, MS 9056, Livermore, CA 94551
seamoor@sandia.gov

1. Introduction

Recent advances in power scaling of continuous wave (CW) rare-earth doped fiber lasers have pushed output powers to 10 kW in the 1 μm regime [1]. Fiber lasers are well suited for high power applications owing to their high electrical-to-optical conversion efficiency, modest thermal loads, and diffraction-limited beam quality, even in large mode area (LMA) multimode gain fibers. These attributes have generated much interest in using fiber lasers as sources for spectral beam combination (SBC). To date, >750 W of near diffraction-limited light has been generated using five 160 W, narrowband, 1063 nm Yb^{+3} -doped fibers spectrally multiplexed with volume Bragg gratings made from photothermorefractive glass [2]. The high dispersion associated with dielectric surface Bragg gratings used for SBC architectures requires that narrowband (<5 GHz) laser sources be used to preserve diffraction-limited beam quality [3]. Similarly, high diffraction efficiencies can only be realized using (reflective) volume Bragg gratings when the bandwidth is limited to ~ 0.25 nm [4], again requiring relatively narrow line width laser sources. Scaling SBC to higher powers will thus require increasing the power of fiber lasers while preserving narrow line width. However, the relatively long lengths of fibers needed for high power lasers (~ 10 -20 m) coupled with the high irradiance of power propagating in the fiber core lower the threshold for detrimental non-linear effects such as stimulated Brillouin scattering (SBS), stimulated Raman scattering (SRS), self-phase modulation, and, in particular, four wave mixing. SBS is often cited as the limiting non-linear process for power scaling, but can often be controlled by increasing the line width of the signal above the SBS bandwidth (~ 200 MHz in silica) [5], increasing the MFD of the fundamental mode [5] and applying strain [6] and temperature gradients [7] to the fiber. Four-wave mixing, however, has proven difficult to control in single-mode fiber lasers, leading to substantially broadened line widths and lower spectral power densities [8]. Using LMA gain fibers and reducing fiber length can increase the threshold for four-wave mixing, but this approach is limited. Currently, narrow line width operation (~ 3 GHz) of Yb^{+3} fiber lasers is limited to 1 kW [1]. Above this power level, line widths typically exceed 2 nm.

To make fiber lasers suitable as sources for SBC it is therefore essential to suppress four-wave mixing, and hence spectral broadening, in single-mode Yb^{+3} -doped fiber lasers. Recent advances in highly dispersive photonic crystal fibers (HD PC fiber) [9] may offer a path forward for generating relatively narrow line width (~ 0.1 nm), high power fiber lasers. We propose a spectrally compressed system consisting of a fiber Raman cavity fusion spliced to a high power, 5-10 kW, Yb^{+3} fiber laser. The Raman cavity is constructed from ~ 10 m of HD PC fiber and two fiber Bragg grating (FBG) pairs, a narrowband (~ 0.05 nm) output coupled partially reflecting FBG and two highly reflective (HR), broadband (2-3 nm) input gratings as shown in (Fig. 3). The spectrally broad (>2 nm) output of a 5-10 kW Yb^{+3} fiber laser is launched into the external fiber Raman cavity and Stokes-shifted via SRS to a wavelength and bandwidth determined by the partially reflecting FBG. As will be shown in Section 2, the extremely high group velocity dispersion (GVD), β_2 , of the HD PCF coupled with the relatively short fiber lengths needed for efficient Raman conversion using high power pump sources disrupt phase matching in the Raman cavity, surpassing four wave-mixing at the Stokes'-shifted wavelength. The bandwidth of the Stokes-shifted light is therefore determined largely by the (narrow) bandwidth of the output coupled FBG. Raman conversion carried out in a HD PCF should therefore increase spectral brightness (W/nm) by more than an order of magnitude at the cost of the quantum defect associated with SRS in silica fibers, or $\sim 6\%$ of the pump energy at 1060 nm. For this approach to be viable, SRS in the Raman cavity must be efficient and the SRS threshold low. To date, Raman conversion efficiencies approaching 94% have been reported in single-mode, step-index fiber Raman cavities [10]. As will be demonstrated in Section 2, Stokes-shifted signals with line widths less than 0.1 nm at 1120 nm and powers approaching 1 kW can be achieved with $>92\%$ efficiency using this approach.

Before undertaking experiments to demonstrate the viability of this approach, it is essential to have a clear understanding of the interplay between and relative importance of the various non-linear processes at play in fibers and how they contribute to spectral broadening. To that end we have

developed a numerical simulator to model Raman conversion and spectral broadening in a fiber cavity that incorporates non-linear processes including four-wave mixing, self-phase modulation, SRS, and SBS, as well as linear processes such as Rayleigh scattering and background loss. In Section 2, as a first step in validating the accuracy of the model, we compare numerical simulations of spectral broadening in a single-mode step-index Raman fiber laser to experimental data taken at the 3-4 W level. The agreement between simulation and experiment, albeit at relatively low power, offers promise that our numerical model is reliable at much higher powers. Section 3 will outline a design for implementing spectral compression in a single high power Yb^{+3} -doped fiber laser “unit” and incorporating several such units into a spectrally beam combined system. We refer to this as spectral compression and combination (SCCC).

2. Theory and numerical simulation

To better understand and anticipate the degree of spectral broadening in a high power fiber Raman laser we developed a comprehensive numerical simulator. The model includes all major nonlinearities at play in a long fiber Raman cavity, such as stimulated Raman scattering (SRS), stimulated Brillouin scattering (SBS), Rayleigh scattering, and nonlinear wave-mixing. The nonlinear wave-mixing processes include self-phase modulation (SPM), cross-phase modulation (XPM), and four-wave mixing (FWM) among numerous longitudinal modes of Raman cavity. The resulting power propagation equation for a single longitudinal mode is given by

$$\frac{dP_i^\pm}{dz} = + \left| \begin{array}{l} -(\alpha_{mat} + \alpha_{RS})P_i^\pm - \alpha_{RS}FP_i^\pm \\ \sum_{k < i} c_{R,(k,i)}(P_k^+ + P_k^-)(P_i^\pm + h\nu_i \Delta v_{spont}) - \sum_{j > i} \frac{\nu_i}{\nu_j} c_{R,(i,j)}(P_j^+ + P_j^- + h\nu_j \Delta v_{spont})P_i^\pm \\ -g_B P_i^\pm P_{i-}^\mp - g_B P_i^\pm h\nu_i \Delta v_{spont} \\ -\frac{2n_2' \omega_i}{c} \left\{ \begin{array}{l} 2 \sum_{l \neq i} \sum_{m \neq i} \sum_{j \neq i} f_{lmji} \sqrt{P_l^\pm P_m^\pm P_j^\pm P_i^\pm} \sin(\Phi_{lmji}) \\ + \sum_{l \neq i} \sum_{j \neq i} f_{ljjl} P_j^\pm \sqrt{P_l^\pm P_i^\pm} \sin(\Phi_{ljjl}) + 2 \sum_{l \neq i} \sum_{m \neq i} f_{liim} P_i^\pm \sqrt{P_l^\pm P_m^\pm} \sin(\Phi_{liim}) \end{array} \right\} \end{array} \right|, \quad (1)$$

where the terms on the right hand side are the material absorption, Rayleigh scattering, SRS, SBS, and FWM, SPM, and XPM. To model continuous-wave light we treated the individual longitudinal modes as random stochastic variables, each of which had as an initial condition a Gaussian stochastic distribution for the amplitude and uniformly randomly distributed phase over $[0, 2\pi]$.

From Eqn. 1 we built a numerical simulator. To confirm the validity of the model and simulator, we compared our simulations with a carefully performed experimental results conducted at the ~3-4W level. In the experiment, we measured the spectral broadening of 1090nm Stokes'-shifted light as a function of pump power for a Raman laser cavity, consisting of a 250 m long HI1060 single-mode fiber, end-pumped with broadband (5nm) 1042 nm source. The Raman cavity was comprised of a 0.5 nm wide 40 % OC FBG and a 5 nm wide 99 % HR FBG. Figure 1 shows the comparison of the spectral broadening between the measured data and the simulation. While the output power at 1090 nm increases from 0.29 W to 3.49 W, the output spectrum also broadens. The excellent agreement between simulation and experiment demonstrates that the model is sound and the simulation is accurate.

In addition to our numerical simulator, we developed an analytical expression for the evolution of the spectral power of each longitudinal mode [11]:

$$\frac{dp_j}{dz} = -\alpha p_j + 4\gamma^2 \int_{z'=0}^z e^{-2\alpha(z-z')} \sum_l \sum_m \sum_n \left\{ p_l p_j p_m p_n \left[\left(\frac{1}{p_l} + \frac{1}{p_j} \right) - \left(\frac{1}{p_m} + \frac{1}{p_n} \right) \right] \times \delta_{j+l, m+n} \cos(\beta_2(\omega_j - \omega_m)(\omega_l - \omega_m)(z - z')) \right\} dz',$$

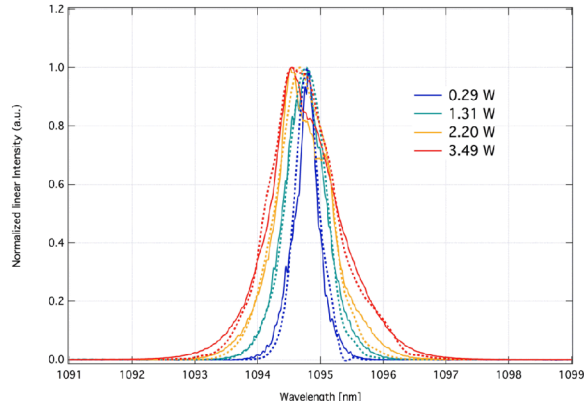


Figure 1. Comparison of the experimental (solid lines) and simulation (dotted lines) results of spectral broadening. The output power varies from 0.29W to 3.49W

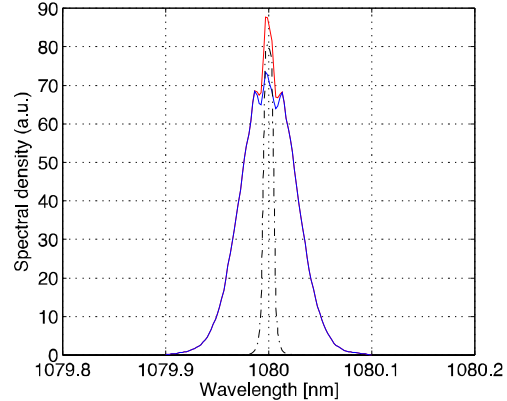


Figure 2. Output spectrum of 975W signal from a highly dispersive Raman fiber laser cavity pumped by 1 kW 1030 nm source.

where p_j is the spectral power density of j^{th} longitudinal mode, α the fiber loss or gain, δ_x the Kronecker delta, β_2 the fiber dispersion, and ω_j the optical angular frequency of j^{th} longitudinal mode. Based on this formula, we further derived the amount of spectral broadening, which is represented by the relative change of peak spectral power density given as

$$\left| \frac{d(\rho_{\text{peak}}(z) / \rho_{\text{peak}}(0))}{dz} \right| \leq 16\gamma^2 P_0^2 e^{-\alpha z} \left(\frac{1 - e^{-\alpha z}}{\alpha} \right) \text{sinc}(\beta_2 \Omega^2 z), \quad (3)$$

where ρ_{peak} is the peak normalized spectral density, P_0 is the initial optical power, and Ω is the rms spectral width. From (3), it is clear that the change of spectral power is a strongly dependent on dispersion and the fiber length and, in particular, that a highly dispersive fiber will significantly reduce the amount of spectral broadening. With this in mind, we have performed a numerical simulation for spectral compression through a Raman fiber laser with a highly dispersive fiber.

Recent advancements in photonic crystal fibers have enabled the development of very highly dispersive fibers with dispersions over -59000 ps/nm/km [9]. We assumed a PCF fiber with a dispersion of -40000 ps/nm/km and mode field diameter of $316 \mu\text{m}^2$. The Raman cavity fiber is 15 m long with 0.03 nm wide OC FBG with 20 % reflectivity at 1080 nm and 1 nm wide HR FBG of 99.9 % reflectivity at 1080 nm. Figure 2 shows the simulation result using a 1 kW, 1030nm, nm linewidth source. The obtained power is 925 W, with spectral bandwidth of 0.0 nm (FWHM). For a comparison, we also performed a simulation based on a 1cm long standard step-index single-mode fiber ($6 \mu\text{m}$ core with -25 ps/nm/km dispersion at 1080 nm), which absorbed the same amount of pump power with the prior simulation. In this case, the spectral broadening at the output end exceeded nm. This simulation result shows that one can spectrally compress a COTS fiber laser, which may have large bandwidth ($>2 \text{ nm}$) with $> 1 \text{ kW}$ single-mode output, into a narrowband ($<0.2 \text{ nm}$) high power output with a small power penalty. This technique enables further spectral combining of such spectrally narrowed sources.

3. Spectral beam combination and compression

The fundamental building block for an SBCC system is a high power, spectrally compressed Yb^{+3} fiber laser as described in Section 1 and shown in Figure 3. The output of a broadband ($\sim 5 \text{ nm}$), 5-10 kW class Yb^{+3} fiber laser is directly spliced to a fiber Raman cavity consisting of three fiber Bragg gratings, two highly reflecting broadband (2-3 nm) input gratings and a partially reflecting output coupling grating, and a highly dispersive photonic crystal fiber (HD PCF). The advantages of an all fiber, monolithic

5-10kW fiber laser

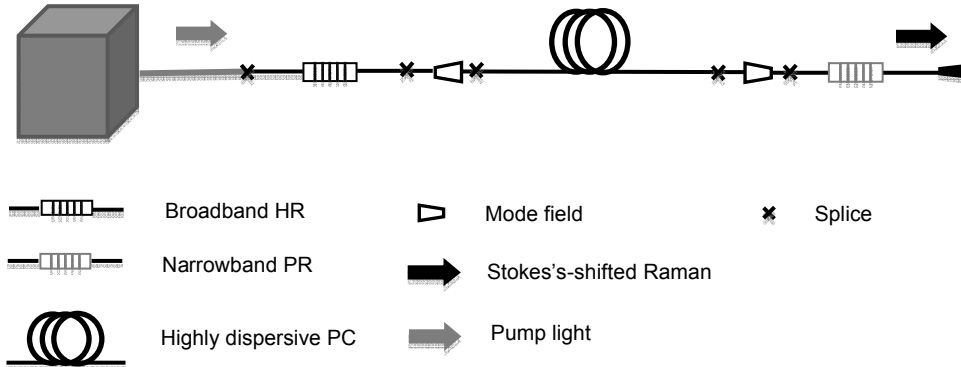


Figure 3. Sketch of spectrally compressed system. HR/PR FBG = highly reflective and partially reflective fiber Bragg grating, respectively

design over free-space coupling include alignment insensitivity, ruggedness, and efficient coupling between the pump source and fiber Raman cavity that avoids the diffraction and reflection losses which typically limit free-space-to-fiber coupling efficiencies to ~80%. Mode field adaptors are spliced between the HD PC fiber and fiber Bragg gratings to compensate for mismatch in mode field diameters between. Two broadband HR FGB's are placed in series to prevent leakage of the Stokes'-shifted light in the external cavity back into the high power pump source. Though the gain of the pump at the Stoke's-shifted wavelength is greater than two orders of magnitude less than at the pump wavelength, feedback from the fiber cavity could induce self-pulsing and instability in the pump and thus should be avoided. The pump power is spectrally compressed and Stokes-shifted ~13 THz to a wavelength determined by the partially reflective, narrowband (~0.05 nm) fiber Bragg grating. The large bandwidth of the Raman gain in silica (~8 THz) allows for Stoke-shifts over ~35-40 nm at 1 μ m with little variation in conversion efficiency. This permits several Yb⁺³ fiber lasers operating at the same wavelength to pump Raman cavities resonate at wavelengths determined by their respective fiber Bragg gratings. Thus, several pump sources operating at similar but not identical wavelengths can be spectrally compressed to wavelengths ideally suited for a particular spectrally beam combined system, eliminating the need for laser sources to run at discretely different wavelengths.

In Section 2 it was determined that a 1kW fiber laser operating at 1 μ m could be spectrally compressed to <0.1 nm with an efficiency exceeding 92%. Several such spectrally compressed "units" can then be multiplexed into a spectrally combined system using a surface Bragg grating or a set of VBG's as depicted in Figure 4. With the linewidths of each SBC unit narrowed from several nm to ~0.2 nm, it is now possible to multiplex several spectrally discrete beams into a single near-diffraction limited beam via SBC. The principle advantage of this approach is that fewer high power laser sources are needed to reach a specified power goal than if the sources were combined using 1 kW, 3 GHz (narrowband) fiber lasers. As an example, to reach 30kW using an array of narrowband 1kW sources, ~35 fiber lasers would be needed after grating losses are taken into account. By contrast, only ~4 spectrally compressed 10 kW laser sources would be needed, greatly simplifying the system architecture improving stability, and lowering cost.

4. Conclusion

We have proposed a fiber laser architecture that we believe offers a path forward to scaling SBC to several tens of kW and possible beyond. The essential building block for this design is a spectrally compressed fiber laser-Raman cavity cell that spectrally compresses the broadband output of a 5-10 kW fiber laser to a bandwidths suitable for SBC. As a tool for future designs, we have developed a comprehensive numerical simulator that models all relevant non-linear processes in fibers that contribute to spectral broadening. Numerical simulations indicate that the 1kW output of a Yb⁺³ fiber laser can be spectrally compressed to < 0.1 nm, implying that fewer broadband laser sources can be spectrally combined to reach a specified power.

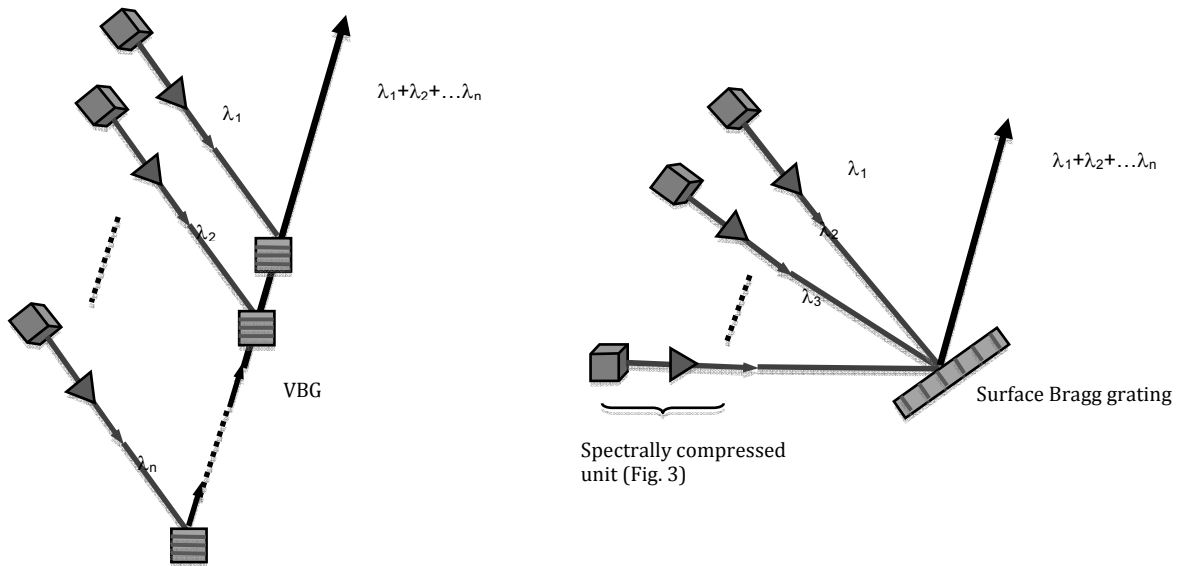


Figure 4. Spectrally beam compressed and combined system using volume Bragg gratings (left) and a surface Bragg grating (right) to multiplex several spectrally compressed high power fiber lasers.

References

- [1] IPG Photonics, <http://www.ipgphotonics.com/>
- [2] "Efficient power scaling of laser radiation by spectral beam combination", A. Sevian, O. Andrusyak, I. Ciapurin, V. Smirnov, G. Venus, and L. Glebov, *Optics Letters*, Vol. 33, No. 4, pp. 384-386, 2008.
- [3] "Spectrally Beam-Combined Fiber lasers for High-Average-Power Applications", T. H. Loftus, A. Thomas, P. R. Hoffman, M. Norsen, R. Royse, A. Liu, and E. C. Honea, *IEEE Journal of Selected Topics in Quantum Electronics*, Vol. 13, No. 3, pp. 487-497, 2007.
- [4] "Modeling of Gaussian beam diffraction on volume Bragg gratings in PTR Glass", I. V. Ciapurin, L. B. and Glebov, V. I. Smirnov, *Proceedings of the SPIE*, Vol. 5742, pp. 183-194, 2005.
- [5] "Nonlinear Fiber Optics", G. P. Agrawal, 2nd Edition, pp. 370-375.
- [6] N. Yoshizawa and T. Imai, "Stimulated Brillouin scattering suppression by means of applying strain distribution to fiber with cabling", *J. Lightwave Technology*, Vo. 11, pp. 1518-1522, 1993.
- [7] J. Hansryd, F. Dross, M. Westland, P. A. Andrekson, and S. N. Knudsen, "Increase of the SBS Threshold in a Short Highly Nonlinear Fiber by Applying a Temperature Distribution", *J. Lightwave Technology*, Vol. 19, pp. 1691-1697, 2001
- [8] V. Khitrov, K. Farley, R. Leveille, J. Galipeau, I. Majid, S. Christensen, B. Samson, and K. Tankala, "KW Level Narrow Linewidth Yb Fiber Amplifiers for Beam Combining", *Proceedings of the SPIE*, Vol. 7686, 2010.
- [9] A. Huttunen, et al., "Optimization of dual-core and microstructure fiber geometries for dispersion compensation and large mode area," *Optics Express* 13(2), p. 627 (2005).
- [10] R. Vallée, E. Bélanger, B. Déry, M. Bernier, and D. Faucher, "Highly Efficient and High-Power Raman Fiber Laser Based on Broadband Chirped Fiber Bragg Gratings", *J. Lightwave Technology*, Vol 24, No. 12, pp. 5039-5042, 2006.
- [11] D. B. S. Soh, J. P. Koplow, S. W. Moore, K. L. Schroder, and W. L. Hsu, "The effect of dispersion on spectral broadening of incoherent continuous-wave light in optical fibers," *Optics Express* 18(21), p. 22393 (2010).

